Korean J. Chem. Eng., **17**(1), 111-117 (2000)

Design for Control: Temperature Uniformity in Rapid Thermal Processor

Ian Huang, Hsin-Heng Liu and Cheng-Ching Yu†

Department of Chemical Engineering, National Taiwan University of Sci. Technol.,
43 Keelung Rd., Sec. 4, Taipei 106-07, Taiwan
(Received 19 October 1999 • accepted 17 December 1999)

Abstract–It is well known that the design of the heating source imposes an inherent limitation on the performance of the rapid thermal processor (RTP). In this work, the similarities and differences between flat and angled reflectors are studied. The *discontinuous* characteristic of the angled reflector can be used to compensate for the edge heat loss of the thin wafer and, consequently, a better temperature uniformity can be achieved. A design procedure is proposed to place the lamp ring as well as the angle of the reflectors. For the control system design, the measurement selection criterion of Huang et al. is employed to find candidate measurement sets followed by a structured singular value criterion. Once the control structure is determined, multivariable temperature controllers are designed according to the internal model control (IMC) principle. From process insight, a fairly simple nonlinear compensation is also devised. Simulation results show that, while only half of the thermal budget is used, improved temperature uniformity can be obtained by using the proposed approach.

Key words: Rapid Thermal Processor, Temperature Control, Temperature Uniformity, Thermal Stress Analysis, Design for Control

INTRODUCTION

Rapid thermal processing (RTP) offers a growing potential as one moves further into the subhalf micron technology [Roozeboom, 1992]. RTP performs single wafer thermal process operations, including annealing, oxidation, nitridation, chemical vapor deposition and cleaning. Moreover, it possesses the feature to significantly reduce the thermal budget while affording single-wafer granularity and cluster compatibility as stated in the National Technology Roadmap. Despite all the promises, the major obstacle for wide-spread applications is inadequate temperature measurement and control [Badgwell et al., 1995]. Therefore, maintaining temperature uniformity over a range of processing conditions is critical for the acceptance of RTP. Notice that temperature uniformity is a prerequisite for within-wafer uniformity. Other factors, such as flow pattern and measurement techniques, which affect uniformity are addressed elsewhere [Roozeboom, 1992]. For a typical RTP system, tungsten-halogen lamps are arranged in linear or pseudo-ring formation [Apte and Saraswat, 1992]. The powers of the lamps are manipulated to control the wafer temperature during the RTP cycle, and it is possible to achieve a wafer temperature ramp rate over 100 ℃/sec. The last decade has seen advances in the modeling, design and control of RTP. The importance of *design* for better temperature control was recognized by several researchers [Apte and Saraswat, 1992; Dilhac et al., 1995; Huang et al., 2000; Norman, 1992; Stuber et al., 1998]. Pseudo-ring lamp arrangement, placement of radiation shield and design of reflectors [Badgwell et al., 1995; Lord, 1988; Sorrell et al., 1990] are proposed to overcome temperature non-uniformity. The design and optimization steps are often carried out on first principle models.

The second factor that affects temperature uniformity is inadequate temperature *control*. The multivariable nature of temperature control is addressed properly by Apte and Saraswat [1992]. Multiloop PID control and Internal Model Control are proposed for the multi-zone RTP systems. Interaction and robustness analyses of multivariable temperature control are also explored by Stuber et al. [1998]. Gain scheduling is also employed to compensate for process nonlinearity as the temperature set point changes. More computationally extensive control techniques such as predictive control and adaptive control are also proposed [Sach et al., 1991].

It is well known that the inherent controllability of a process is generally determined at the design stage and then control can be applied to keep the equipment operating at the achievable performance. The purpose of this work is to compare the performance of RTP systems, and emphasis is placed on temperature uniformity, thermal budget and possible plastic deformation. Applications of interest include nitridation, oxidation and implantation. The remainder of this paper is organized as follows. Section 2 discusses the design aspect of RTP systems. Control structure design and controller synthesis are addressed in Section 3 followed by the conclusion.

DESIGN

In this work, an axisymmetric RTP chamber is studied. A schematic of an RTP system with angled reflectors is shown in Fig. 1. In this system, power is supplied to four rings of tungsten-halogen lamps. Energy is transferred through a quartz window onto

†To whom correspondence should be addressed.
E-mail: ccyu@ch.ntust.edu.tw
This paper was presented at the 8th APCChE (Asia Pacific Confederation of Chemical Engineering) Congress held at Seoul between August 16 and 19, 1999.

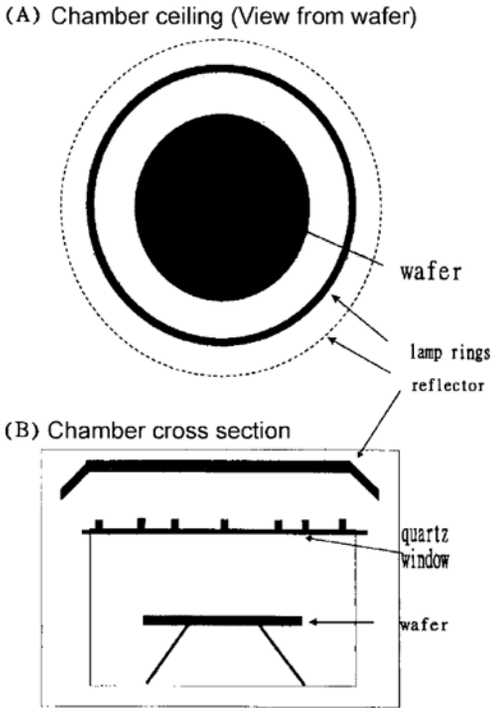

Fig. 1. Schematics of angled RTP.

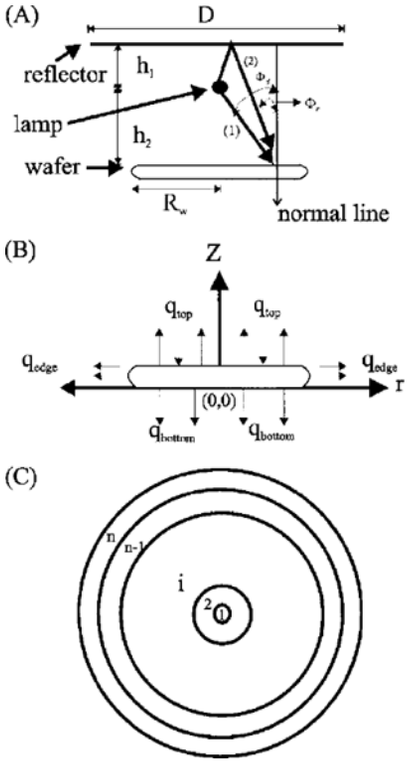

Fig. 2. Modeling of a RTP system.
(A) ray-tracing model, (B) heat transfer between wafer and chamber and (C) discretization of the wafer in the r-direction.

a thin semiconductor wafer via direct and reflective paths.

The RTP system is a typical heat transfer process. However, unlike conventional chemical engineering systems, this is a radiation dominant heat transfer process. Lord [1988] is among the first to model RTP systems. A model for multiple rings configuration, first described by Norman [1992] and later modified by Huang et al. [2000], is adopted here (Fig. 2). This type of model was validated experimentally by several researchers. A cylindrical coordinate is employed to model the temperature on the wafer. The origin of the coordinate system is the center of the wafer bottom surface as shown in Fig. 2B. The following assumptions are made: (1) temperature distribution is axisymmetric, (2) z-direction temperature gradient can be neglected, and (3) no gas-solid reaction occurs. With these assumptions, the differential equations describing the energy balance can be reduced to a one-dimensional (r-direction) model. It can further be discretized into equal-radius annular zones in each of which the temperature (T_i, i=1, ... n) is assumed to be constant (e.g., Fig. 2C). Therefore, we have:

$$\rho_i C_p(T_i) V_i \frac{dT_i}{dt} = -\varepsilon\sigma A_i T_i^4 - hA_i(T_i - T_a) + q^{cond} + \alpha_i \frac{A_i}{2} \sum_{j=1}^{m} S_{ij} P_j \qquad (1)$$

where ρ_i is the density, $C_p(T_i)$ is the heat capacity, V_i is the volume and T_i is the temperature of the wafer in the i^{th} zone. For the radiation heat flux, ε is the total emissivity, σ is the Stefan-Boltzmann constant, A_i is the surface area of the i^{th} zone, α_i is the absorptivity of the i^{th} zone. S_{ij} is the view factor which represents the fraction of energy received by the i^{th} zone from the j^{th} lamp ring, m is the total number of lamp rings and P_j is the power of the j^{th} lamp ring. The ray-tracing model of Gyurcsik et al. [1991] (Fig. 2A) is employed to compute S_{ij} and the angled reflector version was derived by Huang [1997]. For heat convection, T_a is the ambient temperature and, in this work, T_a is taken as the arithmetic mean of the averaged wafer temperature and wall temperature and h_i is the convective heat transfer coefficient. Since the temperatures are relatively uniform, the conduction term q^{cond} generally can be neglected as compared to the other two factors. This is a set of nonlinear ODEs, and the nonlinearity comes from the radiation term.

A cold-wall RTP system with four lamp rings is used to illustrate the interaction of design and control. The chamber geometry is the same as Crowley et al. [1998], but the lamp configuration is re-designed to achieve better temperature uniformity [Huang et al., 2000]. The reflectors are located on the top. The chamber geometry, property of the reflector, lamp ring locations and wafer and system parameters for simulations are summarized in Table

Table 1. System parameters for RTP system

Parameter	Value
Chamber diameter (D, cm)	52
Chamber height (H, cm)	17.5
Distance between reflector and lamp (h_1, cm)	2.5
Distance between lamp and wafer (h_2, cm)	5.0
Wafer diameter ($2R_w$, cm)	20.32
Wafer thickness (δ, cm)	0.0675
Wafer density (ρ, Kg/m^3)	2330
Zone number (n)	30
Emissivity (ε)	0.7
Absorptivity (α)	0.6
Stefan Boltzmann constant (s, W/m^{2}K^4)	5.67×10^{-8}
Relfector reflectivity (R_e)	0.97

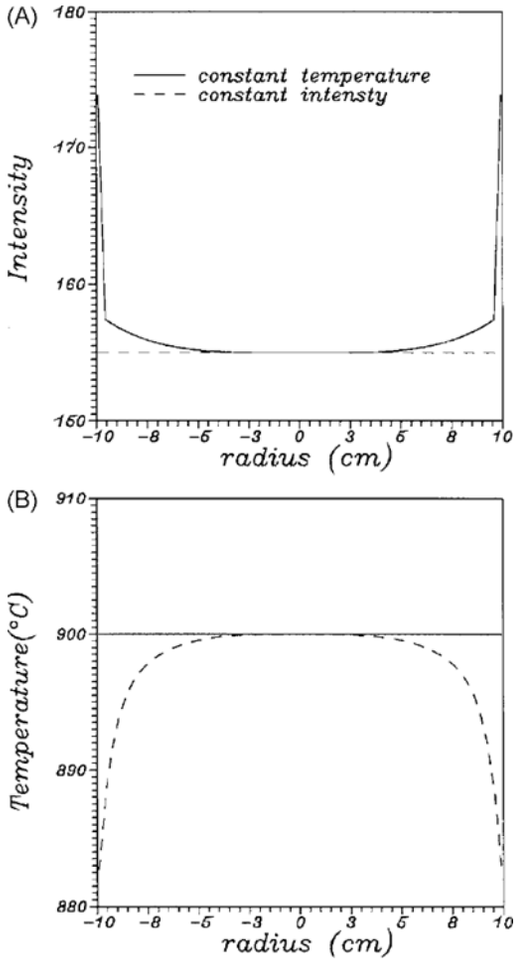

Fig. 3. Intensity and temperature profiles for uniform temperature (solid) and uniform intensity (dashed).

1. In simulation, the wafer is descretized into 30 zones (n=30) and the view factors (S_{ij}) can be derived directly from the ray-tracing model (Fig. 2A). The set of 30 ODE's is solved numerically using the Euler method.

Two types of reflector designs are studied: flat and angled reflectors. For the flat reflector, the design problem is simply to find the lamp ring locations such that the 2-norm between the desired intensity (Fig. 3) and the actual intensity is minimized. The vector of the desired intensity I^d can be found by solving the steady-state version of Eq. (1) by assuming a uniform temperature profile across the wafer (e.g., T=900 ℃). The actual intensity can be calculated from:

$$I=SP \tag{2}$$

where I is the 30×1 vector of intensity, S is the 30×4 matrix of view factor (which is constant for a given design) and P is a 4×1 vector of power input. The optimal power input can be obtained by solving a least square problem. Huang et al.'s [2000] robust design procedure, which takes all possible operating temperatures (400-1,000 ℃) into account, is employed. Four lamp rings are placed at 0, 5, 6, and 16 cm from the center. In terms of temperature uniformity, the result of this four-lamp-ring configuration is almost the same as the three-lamp-ring scheme [Huang et al., 2000]. This clearly indicates the limitation of the flat reflector where the temperature uniformity cannot be improved by adding more lamp rings. Fig. 4A, which shows the intensities from these four lamp rings, reveals that the maximum intensity occurs at r=16 cm for a 20 cm wafer. That means excessive thermal budget is needed to compensate for the edge heat loss. The power input is P_{tot}=7.4 kW/m at 900 ℃. Fig. 5A shows the temperature profile of the optimized RTP design. This corresponds to an averaged temperature deviation of 0.99 ℃ (i.e., ΔT_{avg}=0.99 ℃).

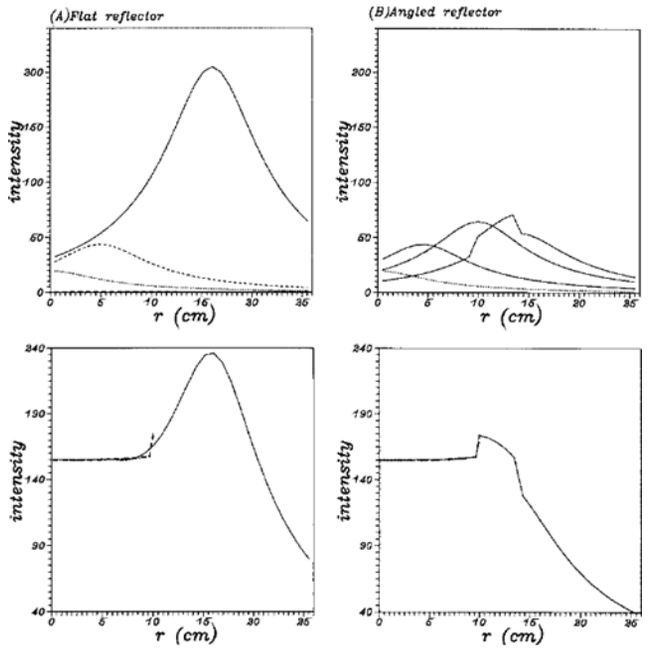

Fig. 4. Desired intensity profile (dashed) and overall intensity profiles for: (A) flat and (B) angled reflectors.

Angled reflectors are sometimes employed in the RTP system. Little is said about the design procedure of the angled reflectors in the literature. Huang [1997] discusses the design of angled reflectors in detail and also derives ray tracing models. In the design, two factors should be taken into consideration: the shape (one-sided or two-sided) and the angle. The study of Huang shows that the one-sided reflector for the outest lamp ring is very effective to compensate for edge heat loss and it is adopted in this work. Therefore, we have one more variable in the design: the angle. The design procedure then becomes: (1) for a given reflector angle, find the optimal lamp ring locations (same procedure as the case of flat reflector), (2) repeat step 1 for different angles and (3) find a reflector angle which gives small averaged temperature deviation as well as thermal budget. This results in a 15 degree angled reflector with lamp ring locations at 0, 4.5, 10 and 14 cm. The top graph of Fig. 4B shows the intensity distributions for each lamp ring. For each lamp ring, the intensity profile is similar to a normal distribution along the r-direction for the flat reflector (e.g., the lamp ring at r=10 cm in top graph of Fig. 4B). Since the lamp ring at r=14 cm has an angled reflector, the intensity profile is no longer a normal distribution (Fig. 4B). This asymmetrical intensity profile can compensate for edge heat loss at a much lower thermal budget as shown in the overall intensity profile (summation of all intensities from different lamp rings) as shown in the

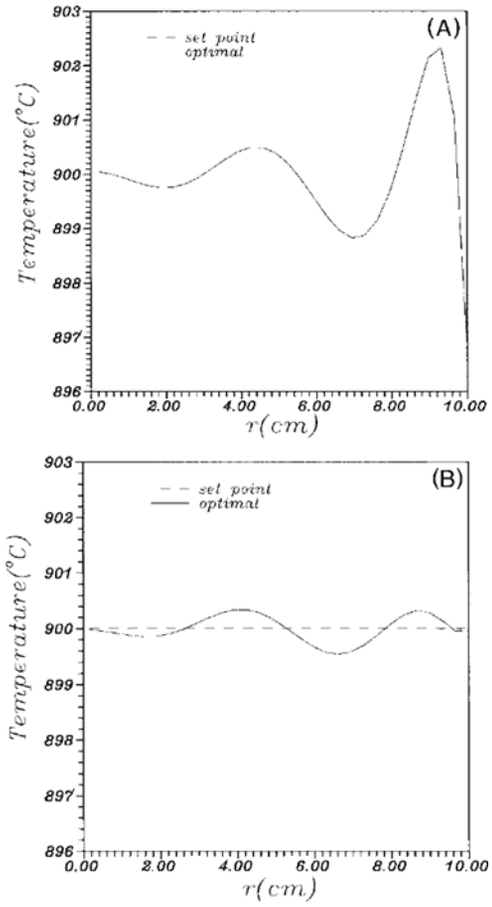

Fig. 5. Desired temperature profile for: (A) flat and (B) angled reflectors.

bottom graph of Fig. 4B. Comparison of Figs. 4A and 4B clearly indicates that the thermal budget (proportional to the total intensity) is much less for an RTP with angled reflectors. The power required is almost 50% less than the case of the flat reflector (P_{tot} =3.8 kW/m at 900 °C). Fig. 5B shows the temperature along the radius direction and it becomes evident that the case of the angled reflector gives better temperature uniformity (e.g., ΔT_{avg} reduced from 0.99 to 0.23 °C) while requiring much less power input.

It should be emphasized that the temperature uniformity is only an *indirect* indicator of process uniformity. For any thermal processes, the thermal stress analysis is important to evaluate whether the temperature non-uniformity exceeds the limit. That is, if the thermal stress exceeds the yield stress, plastic deformation may occur, which leads to defects in the devices [Lord, 1988; Fan and Qiu, 1997; Hebb and Jenson, 1998]. The approach of Hebb and Jenson [1998] is taken here. The wafer is modeled with the following assumptions: it is an isotropic, elastic, flat and thin circular plate free of external forces. Under these assumptions, the thermal stress in the radial and tangential directions can be expressed as [Hebb and Jenson, 1998]:

$$\sigma_r(r)=-\alpha_s E\left[\frac{1}{r^2}\int_0^r T(r)rdr-\frac{1}{R^2}\int_0^R T(r)rdr\right] \quad (3)$$

$$\sigma_\theta(r)=-\alpha_s E\left[T(r)-\frac{1}{r^2}\int_0^r T(r)rdr-\frac{1}{R^2}\int_0^R T(r)rdr\right] \quad (4)$$

where r is the radial position, R is the radius of the wafer, T is temperature, $\alpha_s=4\cdot10^{-6}$ K^{-1} is the thermal expansion coefficient of silicon, $E=1.3\cdot10^{5}$ MPa is the Young's modulus. Using Mohr's circle, the maximum resolved shear stress can be calculated in the plane of the wafer.

$$\tau_s(r)=\frac{1}{2}[\sigma_r(r)-\sigma_\theta(r)] \quad (5)$$

Haasen's model of yield stress of silicon is employed to find the critical stress for plastic deformation [Fan and Qiu, 1997].

$$\tau_{yld}=C\dot{\varepsilon}^{1/m}\exp\left(\frac{u}{n\sigma T}\right) \quad (6)$$

where U=2.3 eV is the activation energy of glide movement, C=45 kPa and m=2.9 are constants, σ is the Boltzmann constant and $\dot{\varepsilon}=4.8\cdot10^{-5}$ s^{-1} is the strain rate and a conservative value is used here. Under the maximum shear stress criterion, it is assumed that a local plastic deformation will occur if the maximum shear stress exceeds the yield stress. Therefore, the stress ratio (τ_s/τ_{yld}) can be used to evaluate the degree of plastic deformation. Comparison is made between the two different designs. In a batch cycle, Fig. 8B shows that the RTP with angled reflector gives a stress ratio less than one throughout the batch cycle. On the other hand, the RTP with a flat reflector (Fig. 8A) has a stress ratio exceeding one. That may lead to defects in dielectric films or degrading of device performance. Again, an RTP with angled reflector shows less thermal stress across the wafer and subsequently leads to fewer possible defects.

The on-going analyses clearly indicate that a better design (angled reflector) can achieve better temperature uniformity while requiring half the thermal budget. It is important to recognize the importance of an improved design for better control performance especially when only a minor modification is required. Moreover, the ultimate performance of a RTP chamber is determined at the design stage.

CONTROL

1. Measurement Selection

Control structure design is important to achieve temperature uniformity [Huang et al., 2000]. That is, we have to determine the controlled variables-temperature measurements. The temperature profile along the radial position plays an important role for the measurement selection. The RTP system uses a linear combination of four lamp powers to match the desired intensity. Notice that each lamp ring has an intensity profile similar to the normal distribution (e.g., Fig. 5). The optimal temperature uniformity corresponds to a unique lamp power combination. The desired temperature profile is a nonlinear function in r and it crosses the temperature set point several times. The profile is similar to a high-order polynomial: $T-T^{set}=\prod_{i=1}^{n}(r-z_i)$ where T^{set} is the temperature set point, n is the number of set point crossings and z_i denotes the location of the set point crossing (zero of the polynomial). Therefore, it becomes clear that the best temperature uniformity which can be achieved is the temperature profile at design, and this is termed the *desired* temperature profile hereafter. Furthermore, the easiest way to maintain this profile is to keep the tempera-

tures already at (or close to) set point (e.g., Fig. 5) under control. This can be interpreted as retaining the shape of the temperature profile by holding several key positions at the set point. Moreover, bringing the temperatures which are not on the set point back to the set point will distort the temperature profile. That is, the temperature profile will not be optimal anymore. This leads to a rather simple measurement selection criterion. Since the temperature profile can be described by a polynomial-like function, possible candidates for temperature control are the "zeros" of the nonlinear function (on the perturbation basis). In the angled reflector case, they are T_1, T_8, T_{16}, T_{24} and T_{29}.

Since we have five set point crossing locations in the desired temperature profile, the measurement selection problem can be simplified from a C(30,4) (27405 alternatives) problem to a C (5,4) (5 alternatives) problem. Therefore, the measurement selection problem is reduced to a manageable size. One approach is to exhaust all possibilities. In theory, all these measurement sets should give ΔT_{avg} fairly close to the best achievable performance. The next step is to check system interaction and inherent robustness by using the structured singular value [SSV, Morari and Zafiriou, 1989]. Table 2 shows the RGA and SSV of the RGA for all five candidate sets. Results from robustness analyses show that the measurement set T_1, T_8, T_{24} and T_{29} gives the most robust multivariable system. Notice that this is the most equal-spaced sensor location from all five possibilities. Physically, this can be understood since the selected measurement locations are the closer to the locations of the maximum intensity of each lamp

Table 2. Averaged temperature deviations, relative gain array and structured singular value for all 5 sets of possible measurement locations

Method	Measurement location	ΔT_{avg} (°C)	RGA	SSV (RGA)
set 1	1 8 16 24	0.25271	8.80 −6.24 41.53 −43.08 −9.62 8.71 −79.77 81.68 2.18 −0.66 58.76 −59.27 −0.35 −0.80 −19.51 24.68	80.496
set 2	1 8 16 29	0.24572	6.91 −8.47 17.78 −15.22 −6.74 12.94 −33.61 28.41 0.89 −3.32 21.67 −18.25 −0.06 −0.15 −4.84 6.05	33.741
set 3	1 8 24 29	0.24246	5.62 −5.69 3.90 −2.83 −4.75 7.66 −6.63 4.72 0.24 −1.01 11.41 −9.64 −0.11 −0.04 −7.68 8.75	19.702
set 4	1 6 24 29	0.24232	2.51 −1.64 0.49 −0.36 −2.13 4.82 −5.33 3.64 0.83 −2.48 14.21 −11.56 −0.22 0.30 −8.37 9.28	22.692
set 5	8 16 24 29	0.24243	3.85 −3.11 0.95 −0.69 −3.84 6.77 −6.09 4.16 1.30 −3.07 14.60 −11.84 −0.30 −0.41 −8.47 9.36	23.701

ring (Fig. 5). That coincides with the common control engineering practice: pair the output with the most influential input. For the case of the flat reflector, in order to avoid process singularity, only three temperatures are controlled (T_3, T_{17} and T_{29}). Therefore, the temperature measurement selection criterion can be summarized as follows [Huang et al., 2000].

(1) Identity the set point crossing locations from the desired temperature profile.

(2) Prefer the approximately equal-spaced rule for placing temperature measurements on these locations.

(3) Check for system robustness, and if the SSV is not acceptable, go back to step 2.

In this procedure, step 1 identifies the potential measurement locations which can achieve temperature uniformity and a smaller subset results. Steps 2-3 deal with the controllability of the square subsystem. Here, engineering judgment (equal-spaced rule) and SSV are employed to ensure the final control structure is not inherently difficult to control.

2. Controller Design

Once the control structure is determined, the next step is to design a multivariable temperature controller. The conventional PID type of controller is preferred for its simplicity and transparency. But, the IMC design principle of Morari and Zafiriou [1989] is employed [Huang et al., 1999]. Since almost half of the batch cycle is involved with ramp type of inputs (e.g., ramp-up and cool down). Type-2 system is considered. For the RTP operated at 900 °C, the m-time-constant model structure gives the following process transfer function matrix:

$$G(s)=K_p \cdot \mathrm{diag}[1/(\tau_i s+1)] \tag{7}$$

where K_p is the steady-state gain matrix and τ_i is the i^{th} time constant. Following the design procedure of Huang et al. [1999], this leads to a diagonal PID type of controller with a static decoupler. Moreover, the diagonal controller has *double* integrators.

$$C(s)=K^{-1}\mathrm{diag}(K_{ii}) \tag{8}$$

where K_{ii} is the diagonal PID type of controller.

$$K_{ii}=K_{c,i}\left(1+\frac{1}{\tau_{I,i}s}+\tau_{D,i}s\right)\frac{1}{s} \tag{9}$$

We term this type of controller as PI^{2}D controller hereafter. The controller parameters can be expressed in terms of IMC filter time constant τ_f.

$$K_{c,i}=\frac{\tau_i+2\tau_f}{\tau_f^2},\ \tau_{I,i}=\tau_i+2\tau_f,\ \tau_{D,i}=\frac{2\tau_i\tau_f}{\tau_i+2\tau_f} \tag{10}$$

Therefore, once the closed-loop time constant τ_f is set, the tuning constants for the PI^{2}D controller can be determined immediately.

In a temperature cycle, the temperature set point can vary by several hundred degrees, which subsequently leads to significant variations in the steady-state gain ($K_{p,ij}$) and time constant (τ_i). For example, $K_{p,ij}$ and τ_i change by a factor of 5 as the temperature set point changes from 900 °C to 400 °C. Intuitively, a nonlinear compensation scheme is necessary to achieve good set point performance. However, the low-order model analysis of

Huang et al. [1999] reveals that since the steady-state gain and the time constant vary with the same factor as the temperature set point changes, the only nonlinear compensation necessary is the reset time of the PI²D controller.

$$\tau_{I,i}=r\tau_i+2\tau_f \tag{11}$$

where r is the ratio of the new temperature set point over the nominal one. In this work, only the reset time, not the controller gain or the decoupler, is adjusted as the temperature set point changes. This is a rather simple and computationally inexpensive nonlinear compensation scheme. The RTP systems with flat and angled reflectors are evaluated by using nonlinear simulations. A fil-

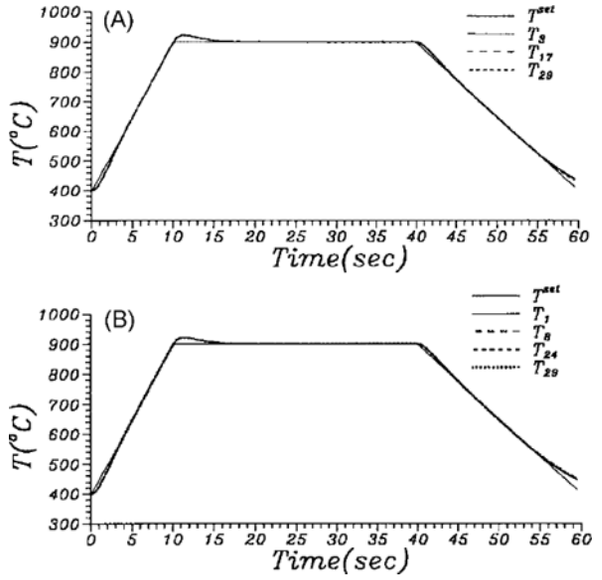

Fig. 6. Temperature responses for the RTP system with τ_f=1.5 sec with (A) flat and (B) angled reflectors.

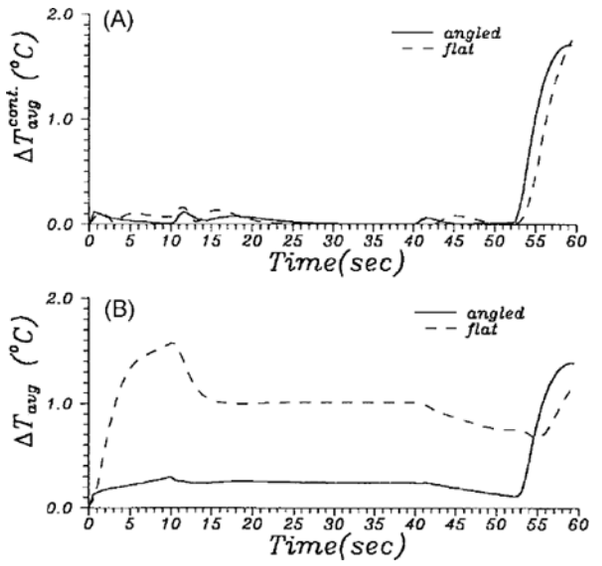

Fig. 7. Averaged temperature deviations of the (A) controlled temperatures and (B) all temperatures using flat and angled reflectors.

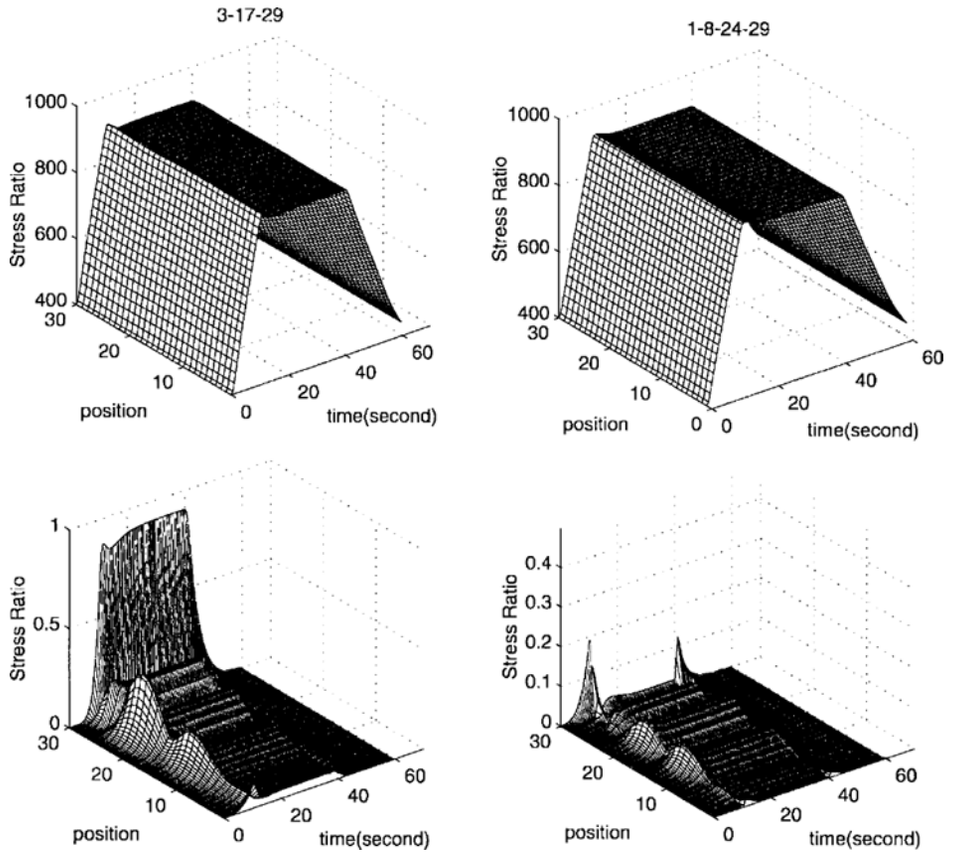

Fig. 8. Dynamic responses of temperatures and stress ratios for: (A) flat and (B) angled reflectors.

ter time constant of 1.5 sec is employed to find the controller parameters. For the controlled temperatures (3 temperatures for the flat reflector and 4 temperatures for the angled reflector), both RTP systems give good set point responses (Fig. 6). However, the temperature uniformity for the case of the angled reflector is significantly improved as illustrated by the averaged temperature deviations for all temperatures (Fig. 7). Results (Fig. 8) show good set point responses can be achieved by using the simplified nonlinear compensation. Again, the low order analytical model offers useful insights in designing the nonlinear compensation element.

CONCLUSION

In microelectronic processing, RTP control systems have the best analogy in process control. In this work, the interaction between design and achievable performance is studied. Results show that an RTP system with angled reflector can achieve better temperature uniformity using only half of the thermal budget as compared to the system of the flat reflector. Moreover, thermal stress analyses show that it can also prevent plastic deformation during a batch cycle held at 900 °C. A complete temperature control design procedure is also given to ensure the desired temperature profile as well as nonlinear compensation. Advantages of the proposed design are illustrated via simulations. More importantly, the performance improvement is achieved with only a fairly simple modification of the reflector.

ACKNOWLEDGEMENT

This work was supported by the National Science Council of Taiwan.

REFERENCES

Apte, P. P. and Saraswat, K. C., "Rapid Thermal Processing Uniformity Using Multivariable Control of a Circularly Symmetric 3 Zone Lamp," *IEEE Trans. Semicond. Manuf.*, **5**, 180 (1992).

Badgwell, T. A., Breedijk, T., Bushman, S. G., Butler, S. W., Chatterjee, S., Edgar, T. F., Toprac, A. J. and Trachtenberg, I., "Modeling and Control of Microelectronics Materials Processing," *Computers Chem. Engng.*, **19**, 1 (1995).

Cho, Y. M. and Kailath, T., "Model Identification in Rapid Thermal Processing System," *IEEE Trans. Semicond. Manuf.*, **6**, 233 (1993).

Crowley, J. L., DeBolski, T. J., Kermani, A. and Lassing, S. E., US Patent 4,755,654 (5 July 1988).

Dilhac, J. M., Nolhier, N., Ganibal, C. and Zanchi, C., "Thermal Modeling of a Wafer in a Rapid Thermal Processor," *IEEE Trans. Semicond. Manuf.*, **8**, 432 (1995).

Fan, Y. H. and Qiu, T., "Analyses of Thermal Stress and Control Schemes for Fast Temperature Ramps of Batch Furnaces," *IEEE Trans. Semiconduct. Manuf.*, **10**, 433 (1997).

Gyurcsik, R. S., Riley, T. J. and Sorrell, F. Y., "A Model for Rapid Thermal Processing: Achieving Uniformity Through Lamp Control," *IEEE Trans. Semicond. Manuf.*, **4**, 9 (1991).

Huang, C. J., Yu, C. C. and Shen, S. H., "Identification and Nonlinear Control for Rapid Thermal Processor," *IEEE Trans. Semiconduct. Manuf.* (revised) (1999).

Huang, C. J., Yu, C. C. and Shen, S. H., "Selection of Measurement Locations for the Control of Rapid Thermal Processor," *Automatica* (in press) (2000).

Huang, I., "Control of Rapid Thermal Processor: Design for Temperature Uniformity," MS Thesis, National Taiwan University of Sci. Technol., Taipei (1997).

Hebb, J. P. and Jensen, K. F., "The Effect of Multilayer Patterns on Thermal Stress During Rapid Thermal Processing of Silicon Wafers," *IEEE Trans. Semiconduct. Manuf.*, **11**, 99 (1998).

Lord, H. A., "Thermal and Stress Analysis of Semiconductor Wafer in a Rapid Thermal Processing Oven," *IEEE Trans. Semicond. Manuf.*, **1**, 105 (1988).

Merchant, T. P., Cole, J. V., Knutson, K. L., Hebb, J. P. and Jensen, K. F., "A Systematic Approach to Simulating Rapid Thermal Processing Systems," *J. Electrochem. Soc.*, **143**, 2035 (1996).

Morari, M. and Zafiriou, E., "Robust Process Control," Prentice-Hall, Englewood Cliff, NJ (1989).

National Technology Roadmap for Semiconductors, Semiconductor Industry Association, San Jose, CA, Dec. (1994).

Norman, S. A., "Optimization of Wafer Temperature Uniformity in Rapid Thermal Processing System," *IEEE Trans. Electron. Dev.*, **39**, 205 (1992).

Roozeboom, F., "Manufacturing Equipment Issues in Rapid Thermal Processing," Academic Press, New York (1992).

Sachs, E., Guo, R., Ha, S. and Hu, A., "Process Control System for VLSI Fabrication," *IEEE Trans. Semicond. Manuf.*, **4**, 134 (1991).

Sorrell, F. Y., Harris, J. A. and Gyurcsik, R. S., "A Globel Model for Rapid Thermal Processors," *IEEE Trans. Semicond. Manuf.*, **3**, 183 (1990).

Stuber, J. D., Trachtenberg, I. and Edgar, T. F., "Desing and Modeling of Rapid Thermal Processing Systems," *IEEE Trans. Semicond. Manuf.*, **11**, 442 (1998).